J Solid State Electrochem (2009) 13:1279–1290
DOI 10.1007/s10008-008-0676-2

ORIGINAL PAPER

Anodic behavior of tin, indium, and tin–indium alloys in oxalic acid solution

Hossnia S. Mohran · Abdel-Rahman El-Sayed · Hany M. Abd El-Lateef

Received: 15 June 2008 / Revised: 6 September 2008 / Accepted: 8 September 2008 / Published online: 23 September 2008

Abstract The anodic behavior of tin, indium, and tin–indium alloys was studied in oxalic acid solution using potentiodynamic technique and characterized by X-ray diffraction and scanning electron microscopy. The *E*/*I* curves showed that the anodic behavior of all investigated electrodes exhibits active/passive transition. In the case of tin, the active dissolution region involves two anodic peaks (I and II) prior to permanent passive region. On the other hand, the active dissolution of indium involves four peaks (I–IV) prior to permanent passive region. The first (I) can be associated with the active dissolution of indium to InOOH, the second peak (II) to the formation of $In(OH)_3$, the third peak (III) to partially dehydration of $In(OH)_3$, and the peak (IV) to complete dehydration of $In(OH)_3$ to In_2O_3. When the surface is entirely covered with In_2O_3 film, the anodic current falls to a small value (I_{pass}) indicating the onset of passivation. The active dissolution potential region of the first three tin–indium alloys involves a net anodic contribution peak, and this is followed by a passive region. It is expected that the investigated peak is related to the formation of In_2O_3 and SnO (mixed oxides). When the formation of oxides (the oxides of In and Sn) exceeds its dissolution rate, the current drops, indicating the onset of passivation precipitation of In_2O_3/SnO and SnO_2 on the surface which blocks the dissolution of active sites. The alloys IV and V showed small second peak at about −620 mV which may be related to oxidation of In to In_2O_3 due to high In content in the two examined alloys. The active dissolution and passive current are increase with increasing temperature for all investigated metals and their alloys.

Keywords Anodic behavior · Tin–indium alloy · Potentiodynamic - Thin film

H. S. Mohran (✉) · A.-R. El-Sayed · H. M. Abd El-Lateef
Chemistry Department, Faculty of Science Sohag,
Sohag University,
Sohag 82524, Egypt
e-mail: hossniamohran@yahoo.com

Introduction

Tin is a moderately corrosion-resistant material widely used in industry in the production of tin can, soft solders, bronze, and dental amalgam [1]. Successful packing of food in cans is greatly dependent upon the unique ability of tin to protect steel from corrosion. The resistance of tinned plate towards corrosion is related to the interrelationship of the characteristics of the can and the product packed there in [2]. Therefore, the corrosion behavior of tin in the presence of fruit acids has attracted much attention [2–9]. According to these studies, the corrosion behavior and properties of the passivating film grown on tin surface strongly depend on the experimental conditions.

Transparent conducting indium (III) oxide thin film coatings are important in solar cells, especially in photovoltaic devices which convert light into electrical energy. Most of the indium oxide and indium tin oxide films have been prepared by a reactive deposition technique in a vacuum deposition unit [10–14], spray pyrolysis [15], and solution growth [16–19]. Several workers have investigated the properties of indium oxide films regarding both their optical transparency and good electrical conductivity. It has been known for many years that indium oxide, as a thin film, is a transparent conductor, typically passing over 90% of visible light and displaying electrical resistivity between 10^{-5} and 10^{-6} Ωm [10].

Physically, these properties result from its being *n*-type semiconductor with a band gap of 3.75 eV [20]. Oxygen vacancies provide electrons by acting as doubly charged donors, and films are generally sufficiently oxygen-deficient. However, the electrochemical properties of indium in electrolyte solutions are rather poorly known. One of the most interesting aspects of anodic oxide films on indium is that they can be reversibly "switched" between electronically insulating and metal conducting states by varying the applied potential. The anodic and cathodic behavior of these films is consistent with their rectification or *n*-type semiconductor properties.

In order to prevent pollution of the environment with lead, the use of lead will be limited in many parts of the world in the near future. In the electronics industry, efforts are now being made to develop a usable lead-free solder, and several tin-based alloys have already been proposed. The goal in the development of lead-free solder is to produce alloys with nearly the same properties as those of lead solder, and most research up to now has focused on melting point and physical strengths of alloys [21]. However, there is little information on the corrosion properties of base alloys for lead-free solder. The metals proposed for lead-free solder are tin–indium alloys. In the recent work, the corrosion behavior of tin-indium alloys and their component pure metals in oxalic acid solution saturated with oxygen is anodically studied. Although the alloys tested are different from those used to lead-free solders in the real world and although the corrosion environments are different from the real environments in which solders are used, a fundamental understanding of corrosion behavior of the lead-free solder alloys has been obtained.

This work aims to investigate the composition of the passive layer formed on the surface of tin, indium, and their alloys under its anodic polarization in oxalic acid solution at different temperatures using X-ray diffraction (XRD) and scanning electron microscope (SEM). The information obtained will allow elucidating the role of the examined acid in the process of the anodic passivation on the investigated surfaces.

Experimental

Materials and solutions

Solutions (0.5 M) of oxalic acid (analytical grade; pH= 2.30) were prepared by dissolving the appropriate weight in doubly distilled water. Tin and indium of high purity (99.999%; Johnson Matthey Chemicals) were used to prepare both Sn and In and Sn–In alloys as disk electrodes (A=0.196 cm^2) in a Gallenkamp muffle furnace using evacuated closed silica tubes at 700 °C for 24 h. The melts were shaken at every 6 h to ensure the homogeneity of melting alloys, and finally, the melts were quenched in ice as previously discussed [22]. Five Sn–In alloys were prepared with the composition as following:

Alloy	I	II	III	IV	V
In (mass %)	0.5	2	5	10	20

The prepared alloys were analyzed using X-ray photoelectron spectroscopy. For each alloy, the percentage of Sn and In was found in accord with the percentage of mixing Sn and In.

Surface characterization

X-ray diffraction of the prepared alloys was carried out using a diffractometer with an iron filter, and copper radiation was used with an accelerating voltage of 30 kV and a filament current of 20 mA. The morphology of Sn and In oxides was examined using scanning electron microscope (JEOL, model 5300).

Electrochemical measurements

The measurements were performed on planar disk electrode embedded in an Araldite holder. Prior to each measurement, the electrodes were polished with sequacious grades of emery paper, degreased in pure ethanol, and washed in running bidistilled water before being inserted in the polarization cell. The reference electrode was a saturated calomel electrode (SCE) to which all potentials are referred. The cell description is given elsewhere [22]. To remove any surface contamination and air-formed oxide, the electrode was kept at −1500 mV (SCE) for 5 min in the tested solution, disconnected and shaken free of adsorbed hydrogen bubbles, and then anodic polarization was recorded by means of potentiostat/galvanostatic (EG&G Model 273) connected with a personal computer (IBM model 30). The potential was altered automatically from open circuit potential up to +1,500 mV ($E_{o.c.p.}$) and at scan rate of 1 mV/s using software version 342C supplied from EG&G Princeton Applied Research.

Each experiment was performed with freshly prepared solution and clean set of electrodes. Measurements were conducted at 30, 40, 50, and 60±0.5°°C for each investigated acid solution. For this purpose, ultrathermostat model Frigiter 6000 382 (SELECTA) was used.

Results and discussion

Behavior of tin electrode

Figure 1 shows the potentiodynamic polarization curves for tin anode in 0.5 M solution of oxalic acid at different

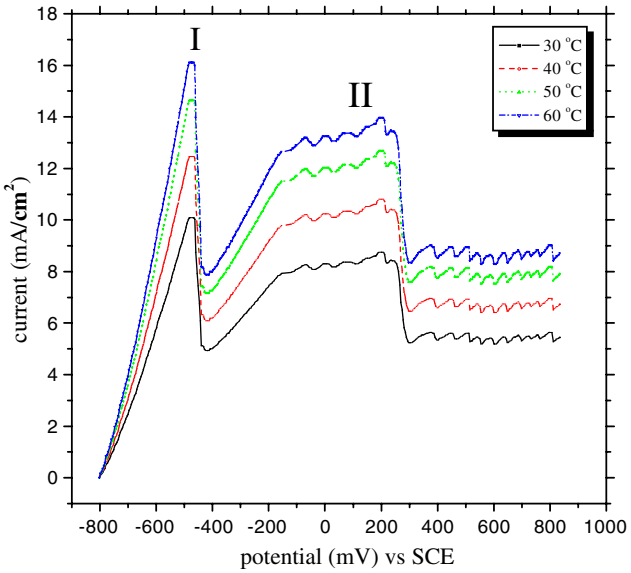

Fig. 1 Potentiodynamic anodic polarization curves of pure tin in 0.5 M oxalic acid solution

temperatures (30–60 °C). The polarization curves were swept from steady state of open circuit potential ($E_{o.c.p}$) up to +1,500 mV vs. SCE. The data reveal that anodic excursion exhibits active–passive transition. The active dissolution region involves two anodic peaks (I and II) prior to permanent passive region. Peak I is well defined at about −474 mV vs. SCE, which can be associated with active dissolution of Sn to Sn(II) species according to the reaction:

$$\mathrm{Sn} \rightarrow \mathrm{Sn(II)} + 2e^{-} \left(E^{\circ}_{\mathrm{Sn2+/Sn^{\circ}}} = -0.136\mathrm{V\ vs.\ NHE}\right) \quad (1)$$

while the broad anodic peak II appearing at about +211 mV vs. SCE is related to electro-oxidation of Sn(II)-containing species according to the reaction:

$$\mathrm{Sn(II)} \rightarrow \mathrm{Sn(IV)} + 2\mathrm{e}^{-} \left(\mathrm{E}^{\circ}_{\mathrm{Sn4+/Sn2+}} = +0.151\ \mathrm{vs.\ NHE}\right). \quad (2)$$

The broad decreasing side of peak II can be attributed to dehydration reaction leading to more stable configuration, arriving at a very well-defined low anodic current plateau which corresponds to the passivity region.

The peak potential (E_p) is slightly shifted to more positive values, while the current peak increases with increasing the temperature. In this solution, the charge transfer reaction occurs in the first active dissolution region (peak I) resulting in the formation of Sn^{2+} ions. Thus, under the prevailing condition, the change is used to produce the following soluble species:

$$\mathrm{Sn} + \mathrm{H_2O} \rightarrow \mathrm{SnOH^{+}} + \mathrm{H^{+}} + 2\mathrm{e}^{-} \quad (3)$$

$$\mathrm{Sn} + \text{ oxalate anion} \rightarrow \mathrm{Sn} - \text{oxalate anion complex} + 2\mathrm{e}^{-}. \quad (4)$$

Gouda et al. [2] reported that SnL_2 species are formed in the case of the oxalate anion. However, when the concentration of complex $SnOH^+$ exceeds the solubility product of $Sn(OH)_2$, the latter precipitates on the electrode surface.

$$\mathrm{SnOH^{+}} + \mathrm{H_2O} \rightarrow \mathrm{Sn(OH)_2} + \mathrm{H^{+}}. \quad (5)$$

Thus, the current drops, suggesting the onset of the primary passivation at a potential comparable with equilibrium potential of the system $Sn/Sn(OH)_2$.

On the other hand, peak II may be due to the conversion of $Sn(OH)_2$ into $Sn(OH)_4$.

$$\mathrm{Sn(OH)_2} + 2\mathrm{H_2O} \rightarrow \mathrm{Sn(OH)_4} + 2\mathrm{H^{+}} + 2\mathrm{e}^{-} \quad (6)$$

$$\mathrm{Sn(OH)_4} \rightarrow \mathrm{SnO_2 \cdot} x\mathrm{H_2O} + (2 - x)\,\mathrm{H_2O}. \quad (7)$$

When the concentration of SnO_2 at the electrode surface exceeds its solubility product, the precipitation of solid oxide occurs on the electrode surface, suggesting that the formation of passive film takes place via a dissolution–precipitation mechanism. When the surface is entirely covered with passive film, the anodic current density falls to a low value (I_p), indicating the onset of the passivation [23].

It is of interest to note that tin hydroxide is thermodynamically unstable with respect to the corresponding oxide [1]. This suggests that dehydration of hydroxide can occur on the tin electrode during the potential sweep to positive direction. The passive layer then becomes more compact and therefore protective. However, the oscillations observed in the polarization curves can be attributed to the competition between the anodic formation and chemical dissolution of the passive oxide film on the electrode surface in the oxalic acid solutions [24].

The present data display that with increasing temperature, the peak current $(I_p)_I$ and $(I_p)_{II}$ are increased, while their corresponding peaks $(E_p)_I$ and $(E_p)_{II}$ are slightly shifted to more positive potentials. It seems possible that the concentration of Sn^{2+} complexes increases with temperature. Accordingly, the concentration of uncomplexed Sn^{2+} decreases. This leads to an increase in the peak currents and to a positive shift in the peak potentials with a simultaneous delay in the passivation, and consequently, the corrosion rate is increased [7]. The fact implies that most of tin dissolves into the solution as tin oxalate anion complex and the passive oxide film must be quite thin [25].

Behavior of indium electrode

Figure 2 shows the potentiodynamic current–potential (*I–E*) curve for indium electrode in 0.5 M solution of oxalic acid

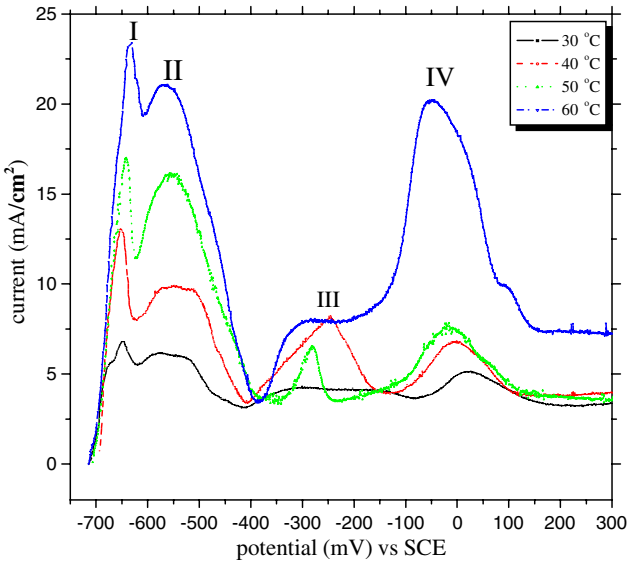

Fig. 2 Potentiodynamic anodic polarization curves of pure indium in 0.5 M oxalic acid solution

at different temperatures (30–60°°C). These curves were also swept from steady state of open circuit potential ($E_{o.c.p}$) up to +1,500 mV vs. SCE (the potential scale of Fig. 2 extended only to +300 mV in order that the peaks are well defined) with scan rate of 1 mV s^{-1}. The anodic sweep exhibits active–passive behavior. The active dissolution region involves four anodic peaks (I, II, III, and IV) prior to the permanent passive region at 30°°C. It is observed that the first anodic peak (I) is located at about −0.648 V vs. SCE, which can be associated with the active dissolution of indium to InOOH according to the reaction:

$$In + H_2O \rightarrow In(OH)_{ads} + H^+ + e^- \quad (8)$$

$$In(OH)_{ads} + H_2O \rightarrow InOOH + 2H^+ + 2e \quad (9)$$

The second peak (II) appears at about −0.559 V, which can be related to formation of $In(OH)_3$ according to the following equation:

$$InOOH + H_2O \rightarrow In(OH)_3, \quad (10)$$

While the third anodic peak (III) is located at −0.287 V, which may be attributed to partially dehydration of:$In(OH)_3$ as the following:

$$2In(OH)_3 \rightarrow In_2O_3 + 3H_2O. \quad (11)$$

The observed peak IV at +0.03 V may be due to completely dehydration of $In(OH)_3$ to In_2O_3. On the other hand, the broad decreasing side of peak IV can be attributed to a precipitation of In_2O_3 on the surface which blocks the dissolution active sites and causes inactivation of a part of the surface with respect to the corrosive medium. When the surface is entirely covered with In_2O_3 film, the anodic current density falls to a small value (I_{pass}), indicating the onset of passivation. These results were confirmed by X-ray diffraction at both the four peaks and passivation potentials, which will be discussed later.

The obtained data reveal that an increase in the temperature results in an increase in the peak currents flowing through the whole range of anodic polarization curve and shifts peak potential (E_p) (except peak IV) to more positive values. It is observed that peak IV shifts to more negative potentials with increasing temperature. On the other hand, the influence of temperature is more remarkable for peak I than that for peak II, especially at higher temperature. It is observed that the variation of temperature has a significant effect on the passivation current through the passive region. In other words, higher passivation current is observed at 60°°C. This behavior could be ascribed to the effect of the chemical dissolution of indium oxide in oxalic acid solution [26]. This is confirmed by X-ray diffraction.

Behavior of Sn–In alloys

Figure 3 shows potentiodynamic *E*/*I* curves of alloy I in 0.5 M solution of oxalic acid at different temperatures; the curves were swept from $E_{o.c.p}$ up to positive potential (+1,500 mV vs. SCE) with scan rate of 1 mV s^{-1}. The anodic excursion exhibits active/passive transition. The active dissolution potential region involves a net anodic contribution peak. This is followed by a passive region.

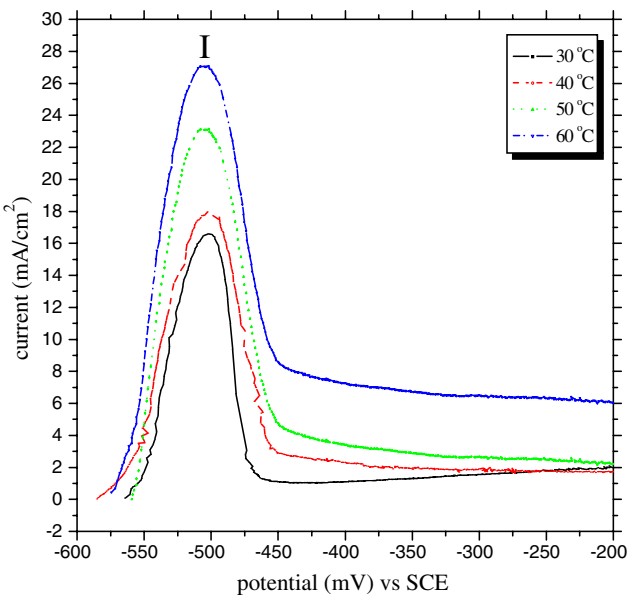

Fig. 3 Potentiodynamic anodic polarization curves of alloy (I) in 0.5 M oxalic acid solution

This region extends up to −200 mV with almost constant current density (I_{pass}). Oxygen evolution was not observed up to +1,500 mV (not represented in Fig. 3), indicating the poor electroconductance of the passive film whose formation and thickening were mainly caused by ionic conductance [27].

In active dissolution region, firstly indium in the alloy dissolves as $[In(OH)_4]^-$ ions as the following:

$$In + 2H_2O \rightarrow In(OOH) + 3H^+ + 3e^-. \quad (12)$$

This reaction is followed by the formation of $[In(OH)_4]^-$ species according to:

$$InOOH + 2H_2O \rightarrow [In(OH)_4]^- + H^+. \quad (13)$$

Further increase of potential in the positive direction leads to the formation of $Sn(OH)_2$ and/or $Sn(OH)_4$. Both $Sn(OH)_2$ and $Sn(OH)_4$ were dehydrated to give the more thermodynamically favorable tin oxides (SnO and SnO_2, respectively) as following:

$$Sn(OH)_2 \rightarrow SnO + H_2O \quad (14)$$

$$Sn(OH)_4 \rightarrow SnO_2 \cdot xH_2O + (2 - x)\,H_2O. \quad (7)$$

At the same time, during the positive going polarization of alloy I in oxalic acid solution, the transformation of a hydrated and ionically conducting indium oxide layer into a more stable crystalline and electronically conducting type of oxide occurs with the loss of water [19].

$$2InOOH \rightarrow In_2O_3 + H_2O. \quad (15)$$

When the rate of formation rate of oxides (indium oxide and tin oxides) exceeds its dissolution rate, the current drops, indicating the onset of passivation due to the precipitation of In_2O_3, SnO, and SnO_2 on the surface which blocks the dissolution of active sites and causes inactivation of a part of the surface toward the corrosive medium [28]. When the surface is entirely covered with mixed oxides from In_2O_3, SnO, and SnO_2 film, the anodic current density falls to the very small value (I_{pass}), indicating the onset of passivation. This suggestion is supported by X-ray diffraction, which will be discussed later.

The data obtained for alloys II and III are similar to those of alloy I. This exhibits that the curves have nearly the same general feature. They are characterized by the appearance of one peak only. Therefore, the observed peak of alloys (I–III) may be attributed to the formation of mixed oxides of both indium and tin as mentioned before. On the other hand, it is observed that the values of anodic peak current are different from the first three investigated alloys compared with pure tin in the same conditions. These behaviors indicate very interesting results that indium content in the Sn–In alloy plays an important role in the active dissolution of Sn in oxalic acid solution.

Alloys IV and V exhibit different behavior compared to the first three alloys (Fig. 4). The curves of alloys IV and V show two peaks: the first at potential of about −616 and −620 mV, the second at −498 and −507 mV, respectively (nearly at the same potential in the case of alloys I–III). However, the data reveal that the anodic current of peak I is very small compared to that of peak II. On the other hand, it is observed that peak I becomes clearer at higher temperature. This peak may be attributed to the formation of small amounts from In_2O_3.

Figure 5 shows comparison between the potentiodynamic anodic polarization curves of Sn and Sn–In alloys at 30°°C in 0.5 M solution of oxalic acid. These curves reveal that the addition of indium to Sn up to 5% In leads to an increase in the peak current in the case of alloys I and II (0.5 and 2.0% In, respectively) compared with the current of Sn, while the peak current in the case of alloy I is higher than that of alloy II. This behavior may be due to the presence of In as a minor element in the alloy I, enhancing the dissolution current and leading to an increase in the peak current [29]. However, as a result of increasing In content in the alloy, peak current starts to decrease and reaches a lower value in the case of alloy III (5.0% In) compared to that of pure tin. These results show that the presence of In at certain percentage (5.0% In) in Sn–In alloy decreases the anodic corrosion current of the alloy compared with that of pure tin and hence improves its

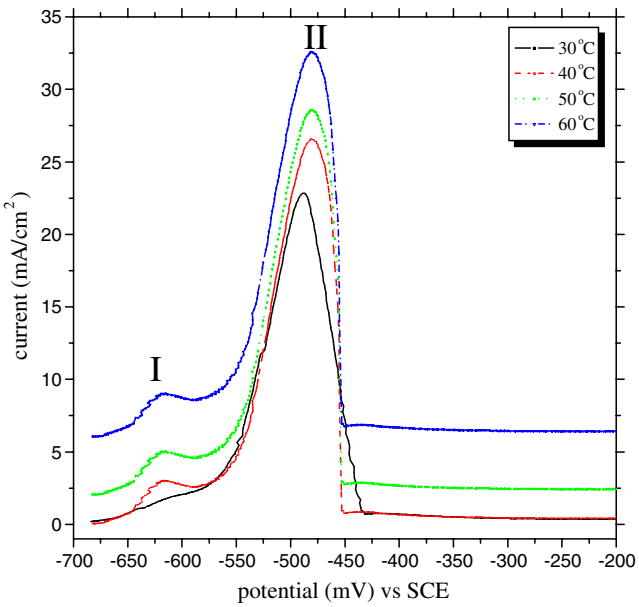

Fig. 4 Potentiodynamic anodic polarization curves of alloy (V) in 0.5 M oxalic acid solution

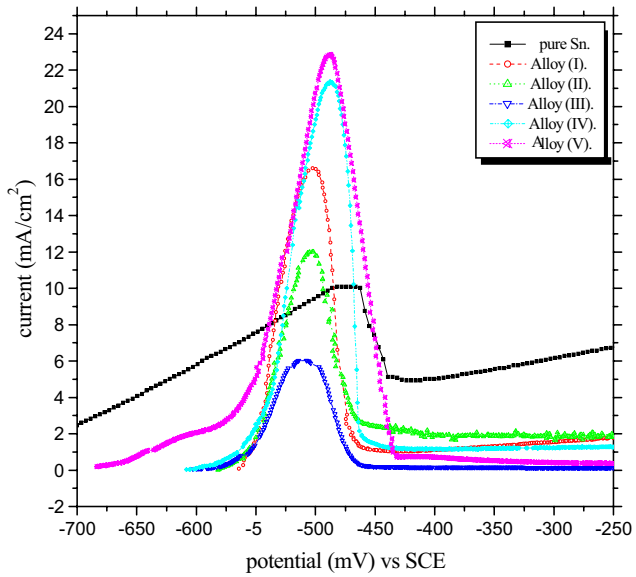

Fig. 5 Comparison between potentiodynamic anodic polarization curves for Sn and its Sn–In alloy in 0.5 M oxalic acid solution at 30 °C

stability against corrosion. This behavior indicates the beneficial effect of the In content (at 5.0% In) in the alloy.

The results show that the peak potential shifts to more negative values for the first three alloys compared with pure tin. This negative shift is probably due to the existence of both In/In_2O_3 and Sn/SnO_2 systems, and this potential value can be considered to be a mixed oxide involving both systems [22]. However, by comparing the potentiodynamic polarization curves in Fig. 5 of alloy IV with those pure tin, it is observed that the peak current of alloy IV is higher than that of pure tin and reaches maximum value in the case of alloy V (20.0% In). In addition, a very small peak is obtained at about −616 and −620 mV (close to the starting anodic polarization), in addition to that mentioned above at −498 and −507 mV, respectively, in the case of alloys IV and V. The results also show that the peak potential of alloy IV and V shifts to more positive values compared with the first three alloys. This behavior confirms that the tendency of the two mentioned alloys (IV and V) towards passivity decreases with increasing indium content.

Comparing peak current (I_p) of Sn–In alloys, it is found that I_p gradually decreases with increasing In content until 5.0%, then I_p increases with further increasing indium in the alloy. This behavior can be correlated to the formation of two phases. X-ray confirmed that γ-phase (γ-$InSn_4$, tetragonal, less surface area) is formed with increasing indium until 5.0%, while β-phase (β-In_3Sn, hexagonal, more surface area) with more than 5% indium content in the alloys (IV and V). Accordingly, the corrosion rate in the active region (peak current) decreases as an increase in indium content in the alloy up to 5.0%, then starts to increase above 5.0% In. These results are similar to those obtained by Lee et al. [30] and Che et al. [31]. They reported that the alloys with less than 10.0% In show the maximum in the intermediate state thermal resistivity.

It is observed that the current density of the passive region sharply decreases in the investigated Sn–In alloys compared with that in pure tin. These results suggest that the alloy surface is well protected most probably by the formation of slightly porous anodically formed films of mixed oxides from both In and Sn oxides [22], and the dissolving power of oxalic acid on these oxides is very weak. Furthermore, it can be assumed that the presence of indium as alloying element decreases the active sites density in the oxide film and consequently decreases the rate of complex formation with oxalic acid anions adsorbed at the alloy oxide surface.

The data exhibit that the peak currents and the passivation currents increase with an increase in temperature in all investigated alloys. Furthermore, the peak potentials shift towards more positive as an increase in temperature. The values of log peak current (I_p) for various temperatures were plotted versus $1/T$ (K^{-1}) in Fig. 6. The Arrhenius plot for I_p furnishes apparent activation energy values (E_a) for electrochemical process of both pure tin and its investigated alloys. The apparent activation energy seems to be around 14±0.30 kJ/mol for pure tin and alloy I. This result suggests that the low content of indium in alloy I does not alter appreciably the dissolution rate of tin. On the other hand, the activation energy increases to around 22.5±0.6 kJ/mol with increasing indium content in alloys II, III, and V. This observed that the higher energy barrier

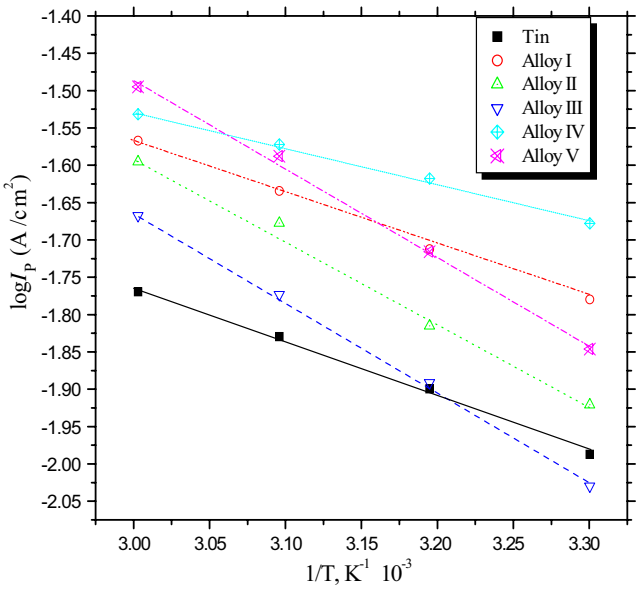

Fig. 6 Arrhenius plots for tin and tin–indium alloys corrosion in 0.5 M oxalic acid solutions

would be attributed to the hindrance of dissolution process by increasing indium contents in the latter alloys. The observed paradox in the low energy barrier determined, in the case of alloy IV compared with that in the pure tin and other investigated alloys, may be attributed to the onset of hexagonal β-phase providing more active sites for dissolution at the electrode surface of alloy IV.

Composition and properties of anodic passive film

X-ray diffraction

The composition of the passive film formed on the surfaces of Sn, In, and some investigated alloys after anodic potentiostatic polarization treatment in 0.5 M oxalic acid solutions for 20 min at different formation potentials was examined. The passive electrode was withdrawn carefully, washed with doubly distilled water, dried, and finally examined by X-ray diffraction. The data for the composition nature of passive film formed at peak potential of Sn electrode (−474 mV vs. SCE) in 0.5 M oxalic acid confirm the existence of Sn as a major and SnO as a minor constituent. These results indicate that the peak potential of tin in oxalic acid solution is related to the formation of SnO on the electrode surface. In addition, X-ray diffraction data for peak II (at +211 mV) indicate that the surface contains small amounts of SnO/SnO_2. These data support our suggestion that peak II of Sn is related to the formation of SnO/SnO_2 system on the electrode surface, while the data obtained for tin electrode treated at +1,500 mV (passive region) exhibit that the surface contains very small amounts of SnO and large amounts of SnO_2. This indicates that SnO_2 is more predominant. In addition, there are not any data of XRD related to the presence of Sn metal in this region. This indicates that the Sn surface is completely covered by mixed oxides film of SnO and SnO_2.

X-ray data for indium electrode, treated potentiostatically at first peak potential (−646 mV), indicate that the surface contains In and InOOH. This confirms that the first peak (I) may be attributed to InOOH formation on the indium surface. However, the data for indium electrode, treated at −559 mV (second peak), show that the surface contains In, InOOH, and $In(OH)_3$. This indicates that the surface is covered by mixed oxides of $InOOH/In(OH)_3$, and the amount of $In(OH)_3$ is higher compared with that of InOOH at this investigated peak potential. The data for the composition nature of the passive film formed at the third peak potential of indium (−287 mV) confirm the existence of In and $In(OH)_3$ as minor constituents and In_2O_3 as a major one. These data support our suggestion that the investigated peak potential (III) is related to the formation of $In_2O_3/In(OH)_3$ on the electrode surface. The data at peak IV (at +30.0 mV) indicate that the surface contains In and In_2O_3 only. This result confirmed that peak potential (IV) is related to the conversion of $In(OH)_3$ into In_2O_3, while the data obtained at +1,500 mV (passive region) show the existence of In_2O_3 only. This indicates that In surface is completely covered by a thick oxide film of In_2O_3. This trend may be attributed to direct oxidation of In to In_2O_3 in the passive region, in addition to the In_2O_3 which is formed at peak IV.

X-ray data for alloy III (5.0% In), treated potentiostatically at peak potential (−507 mV; Fig. 7), indicate that the surface contains large amounts of Sn and SnO and small amounts of SnO_2 and In_2O_3. This indicates that the oxidation of Sn to SnO is more predominant at the peak potential formed (−507 mV), with the presence of small amounts from SnO_2 and In_2O_3. The data for alloy III treated at +1,500 mV (passive region) reveal that the surface is covered by oxides SnO_2 and In_2O_3 as major constituents and In_2SnO_5 as a minor one. The formation of In_2SnO_5 oxide may take place due to the interaction

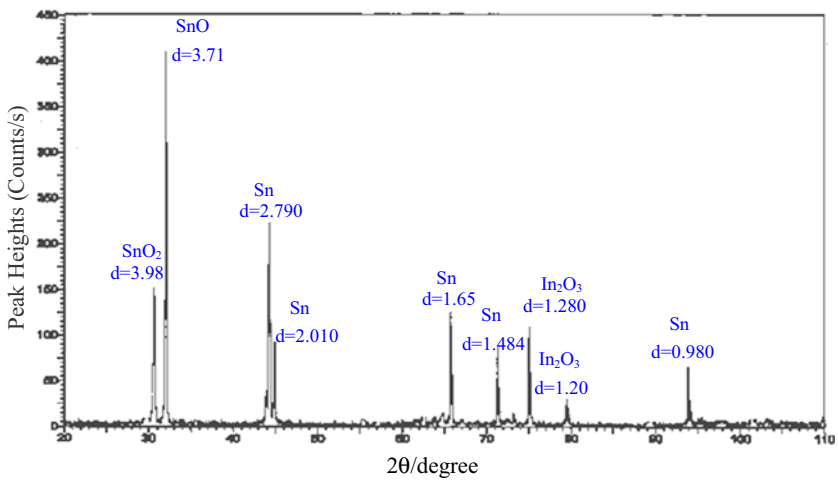

Fig. 7 X-ray diffraction pattern for the passive film on alloy III (5.0% indium) surface formed anodically in 0.5 M oxalic acid solution at applied potential −507 mV (at peak I)

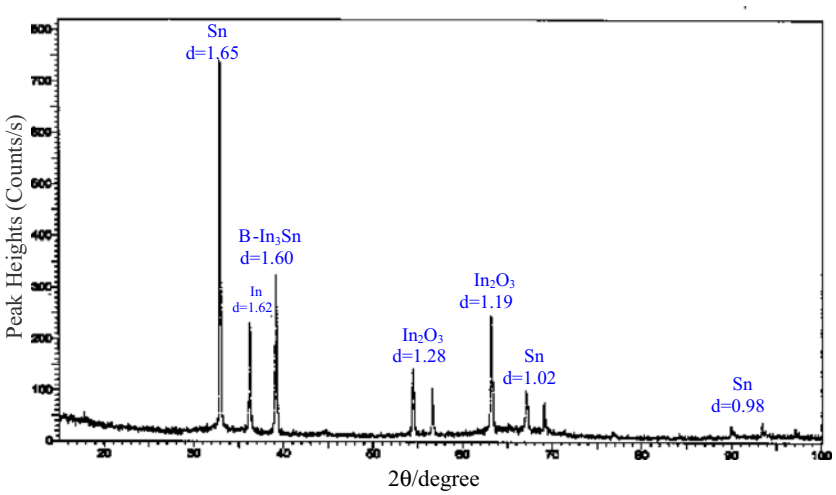

Fig. 8 X-ray diffraction pattern for the passive film on alloy V surface formed anodically in 0.5 M oxalic acid solution at applied potential −625 mV

between In_2O_3 and SnO_2 at the passive region according to the following equation:

$$In_2O_3 + SnO_2 \rightarrow In_2SnO_5. \quad (16)$$

The data in Fig. 8 for the alloy (V; 20% indium) treated potentiostatically at −625 mV vs. SCE (peak I) in 0.5 M oxalic acid solution at 60 °C reveal that the surface contains Sn, β-In_3Sn, and small amounts of In_2O_3. This result implies that the peak potential at −625 mV vs. SCE may be attributed to In oxide formation (In_2O_3) on the alloy surface. This indicates that the high indium content in the alloy (20.0% In) leads to the appearance of this peak which is attributed to the formation of In_2O_3. However, the data of the same alloy, treated at −487 mV (peak II; Fig. 9), show that the surface is partially covered by SnO in large amount and by SnO_2 and In_2O_3 in small amounts. Accordingly, the data reveal that the peak potential (II) of alloy V is related to the formation of SnO/SnO_2 and In_2O_3 on the electrode surface. The data for the same alloy (V) treated at +1,500 mV (passive region; Fig. 10) reveal that the surface is covered by In_2O_3 as a major and SnO_2 as a minor constituent, in addition to very small amounts from In_2SnO_5 oxide. This behavior indicates that the existence of indium in large amounts in the alloy (20.0% In) leads to In_2O_3 formation in a large amount at the surface and becomes more predominant. Therefore, the formation of In_2O_3 on the alloy surface firstly retards the oxidation of Sn to SnO_2, and accordingly, the formation of tin oxides (SnO_2) on the alloy surface is reduced.

Microscopic examination

Figure 11a–d shows the micrographs of the anodic passive film formed potentiostatically on surface of indium in 0.5 M oxalic acid solution at applied potentials −648, −559,

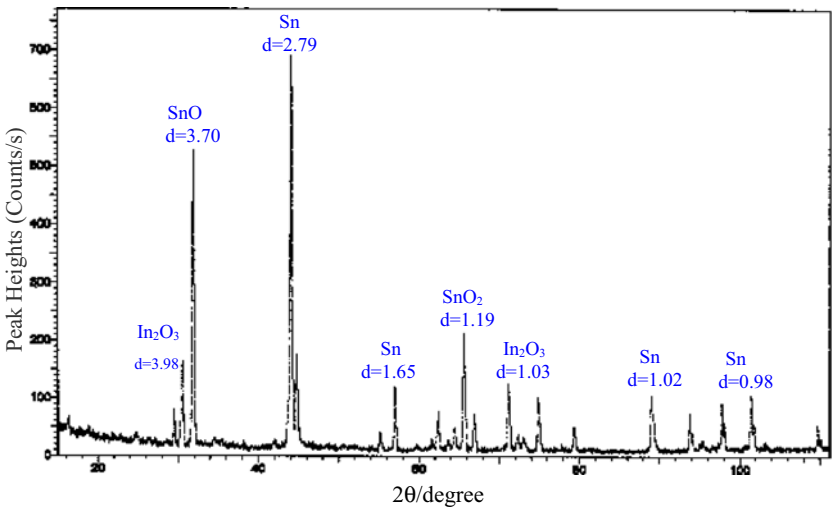

Fig. 9 X-ray diffraction pattern for the passive film on alloy V surface formed anodically in 0.5 M oxalic acid solution at applied potential −487 mV (at peak II)

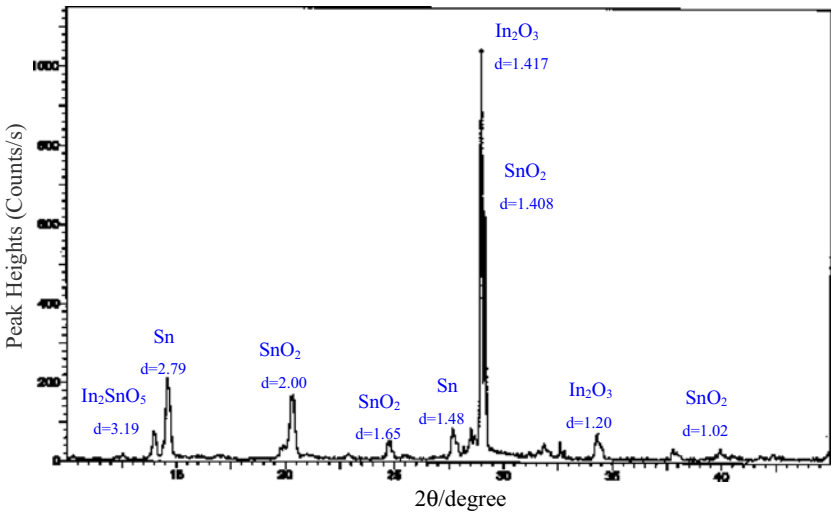

Fig. 10 X-ray diffraction pattern for the passive film on alloy V surface formed anodically in 0.5 M oxalic acid solution at applied potential +1,500 mV (at passive region)

−287, and +1,500 mV with a magnification of 2,000×. It may appear from Fig. 11a that the surface is partially covered by the passive film that the electrode surface may be seen. One layer is observed on the electrode surface. The crystals of the layer exhibit different shapes. The crystals of this layer are not compact, i.e., there are vacancies between them. These observations are in agreement with the data of X-ray diffraction that the layer is related to InOOH. Figure 11b suggested that in SEM photographs of In treated at −559 mV, the surface is almost completely covered by the passive layer. Two layers are observed on the electrode surface. The crystals of the upper layer exhibit different shapes, and the crystals of this layer are not compact. Underneath the upper layer, the second later formed layer

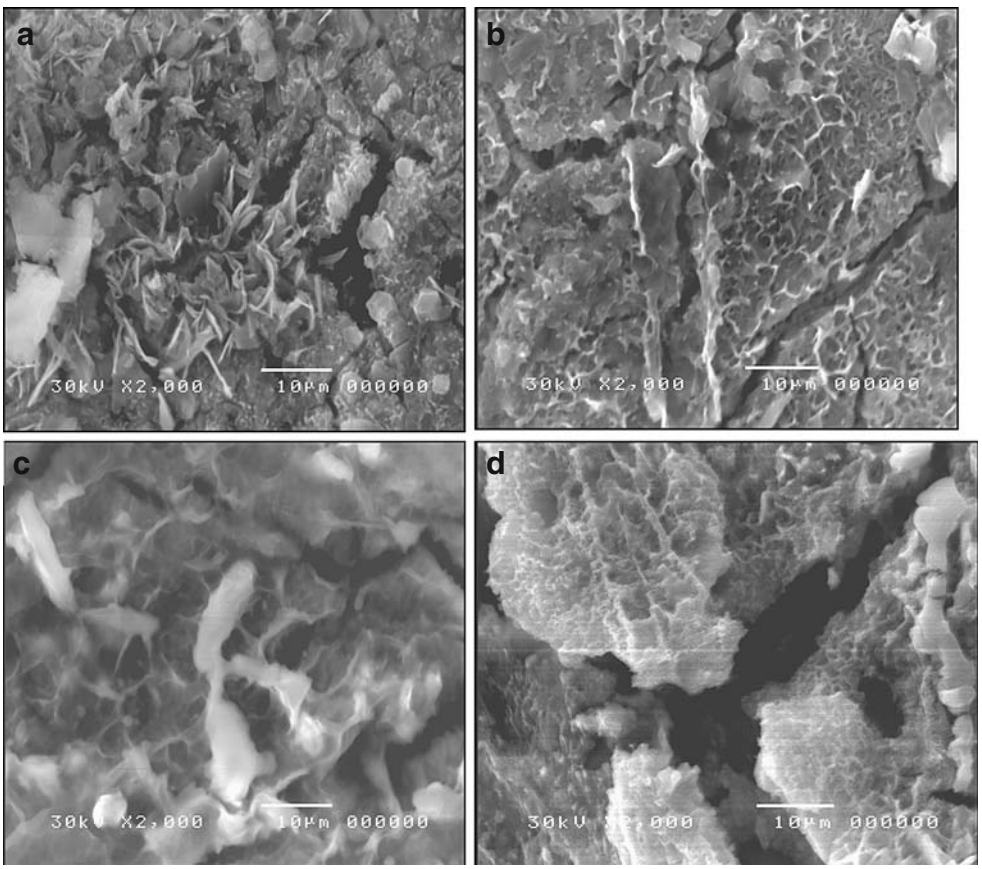

Fig. 11 SEM photographs of passive film on the indium surface formed anodically in 0.5 M oxalic acid solution at magnification 2,000× at **a** −648 mV, **b** −559 mV, **c** −287 mV, and **d** +1,500 mV

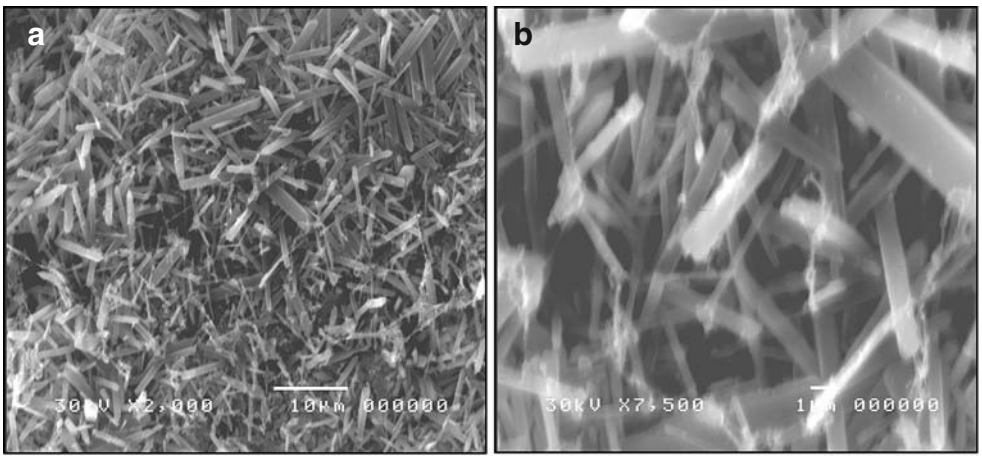

Fig. 12 SEM photographs of passive film on the tin surface formed anodically in 0.5 M oxalic acid solution at +1,500 mV **a** at magnification 2000× and **b** at magnification 7500×

appears, but it seems to lie below that observed at the upper layer. These observations are in agreement with the data of X-ray diffraction that the upper layer is related to InOOH, while the underneath layer is due to $In(OH)_3$ formation. However, the photograph of In treated anodically at −287 mV (more positive potential) given in Fig. 11c recognized that the quantity of $In(OH)_3$ crystals at the upper layer is less than that observed in Fig. 11b (at more negative potential) and the crystal size is smaller. The vacancies between crystals become wider so that the crystals of the underneath layer appear easily through them. In addition, the amount of crystals of the underneath layer are much greater compared with the same layer formed at −559 mV. Therefore, the electrode surface seems to be completely covered by $In(OH)_3$ and In_2O_3, as confirmed by X-ray diffraction. For In electrode surface treated at +1,500 mV (Fig. 11d), it seems that one layer on the electrode surface and surface emerges as caves; however, the quantity of oxide crystals increased and set greater in size, and the electrode surface is completely covered by In_2O_3.

Figure 12a,b shows the micrographs of the anodic passive film formed potentiostatically on the surface of Sn in 0.5 M oxalic acid solution at applied potential +1,500 mV with a magnification of 2,000× and 7,500×. It may appear from Fig. 12a at magnification 2,000× that the surface of electrode is completely covered by the passive oxide film so that the electrode surface cannot be seen. Two layers are observed on the electrode surface (double nature). The quantity of the oxide crystal in the underneath layer increases and becomes more compact, whereas the crystals of the upper become loosely bound to the metal surface and are lost in the bulk of the solution so that SnO_2 is more predominant at high anodic potential. These observations are in agreement with the data of X-ray diffraction that the upper layer is related to SnO, while the underneath layer is due to SnO_2 formation. Figure 12b suggested the different shapes of Sn oxides at high magnification (7,500×) where the shapes of the crystals are clearer.

Figure 13a,b shows the micrographs of the anodic passive film formed potentiostatically on surface the of

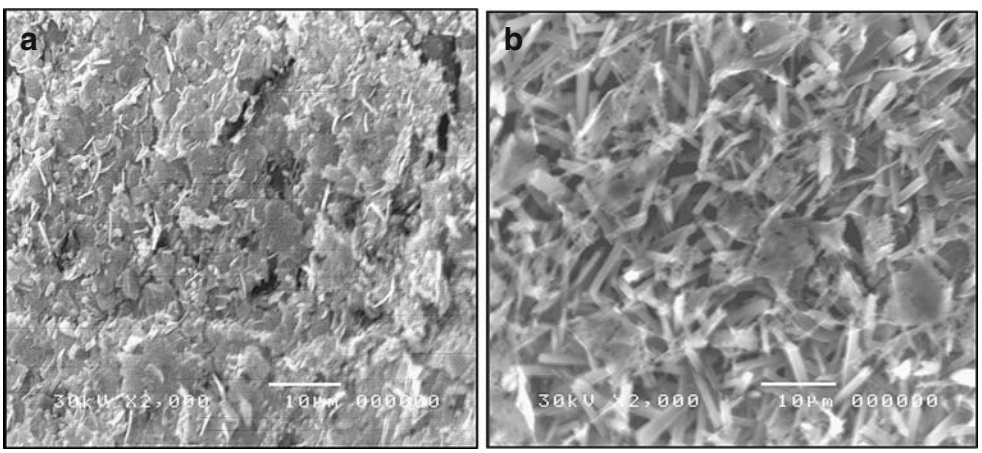

Fig. 13 SEM photographs of passive film on the alloy V (20% indium) Surface formed anodically in 0.5 M oxalic acid solution at magnification 2,000× **a** at −30 mV and **b** at +1,500 mV

alloy V (20% indium) in 0.5 M oxalic acid solution at applied potentials (−30 and +1,500 mV). It would be recognized from Fig. 13a that the surface is covered by few oxide crystals In_2O_3 and very small particles may be SnO. The surface of that alloy treated at +1,500 mV recognized that the concentration of Sn oxide crystals is higher compared with the last sample treated anodically at lower anodic potentials. The particles of the upper layer are rendered closer and much bigger in size and cover most of the electrode surface. This result suggests that the formation of SnO_2 is more pronounced at high anodic potentials. The particles of the underneath layer can still be identified, but its concentration is very low. Moreover, it is suggested that the formation of indium oxide on the alloy surface retards the oxidation of Sn to SnO_2.

Conclusions

1- Tin electrode showed two anodic peaks, while indium showed four anodic peaks, and the first three alloys exhibited only one peak. Alloys IV and V revealed two anodic peaks, the first peak may be corresponding to the formation of In_2O_3, and the second to the formation of In_2O_3 and SnO (mixed oxides).

2- Addition of In to Sn up to 5% leads to an increase in the peak current in the case of alloy I which is higher than that of alloy II. This behavior may be due to the presence of indium as a minor element in the alloy I, which promotes the dissolution current and leads to an increase in the peak current. However, as a result of increasing indium content in the alloy, peak current starts to decrease and reaches lower value in the case of alloy III (5% In) compared to that of pure tin. This result exhibits that the presence of In at certain percentage (5% In) in Sn–In alloy decreases the anodic corrosion currents of the alloy compared with that of pure tin and hence improves its stability against corrosion.

3- X-ray diffraction and SEM micrographs confirmed that the oxide film formed on the tin surface and polarized at −474 mV (peak I) contains small amount of SnO. Then, at +211 mV (peak II), SnO/SnO_2 system is formed, while at +1,500 mV (passive region), the surface is completely covered by mixed oxide films of SnO and SnO_2. The surface of indium polarized at potential of peak I is found to contain InOOH, and at peak II, $InOOH/In(OH)_3$ system is formed. The oxide film formed at peak III consists of $In(OH)_3$ as a minor and In_2O_3 as a major constituent. X-ray data at peak IV indicate that the surface is partially covered by In_2O_3 in small amounts. The data obtained at +1,500 mV (passive region) show the existence of In_2O_3 only in a large amount. The data for alloy III (5% In) treated at peak potential (−507 mV) indicate that the surface contains large amounts of both SnO and In_2O_3. The data for the same alloy treated at +1,500 mV (passive region) reveal that the surface is covered by oxides of SnO_2 and In_2O_3 as a major constituents and In_2SnO_5 as a minor one.

References

1. Gannetti BF, Sumodjo PT, Rabockai T, Souza A, Barboza J (1992) Electrochim Acta 37:143. doi:10.1016/0013-4686(92)80023-F
2. Gouda V, Rizkalla E, Abd El Wahab S, Ibrahim E (1981) Corros Sci 21:1. doi:10.1016/0010-938X(81)90058-5
3. Tselesh AS (2008) Thin Solid Films 516:6253. doi:10.1016/j.tsf.2007.11.118
4. Blunden S, Wallace T (2003) Food Chem Toxicol 41:1651. doi:10.1016/S0278-6915(03)00217-5
5. Almeida CMVB, Giannetti BF (2001) Mater Chem Phys 69(1–3): 261
6. Jafarian M, Gobal F, Danaee I, Biabani R, Mahjani MG (2008) Electrochim Acta 53:4528. doi:10.1016/j.electacta.2008.01.051
7. Dezhi L, Paul PC, Changqing L (2008) Corros Sci 50:995. doi:10.1016/j.corsci.2007.11.025
8. Seruga M, Metikos-Hukovic M (1992) J Electroanal Chem 334:223. doi:10.1016/0022-0728(92)80574-N
9. Giannetti BF, Sumodjo PT, Rabockai T (1990) J Appl Electrochem 20:672. doi:10.1007/BF01008881
10. Bellingham JR, Phillips WA, Adkins CJ (1991) Thin Solid Films 195:23. doi:10.1016/0040-6090(91)90255-V
11. Schumacher LC, Momiche-Afara S, Leibovitch M, Dignam MJ (1988) J Electrochem Soc 135:3044. doi:10.1149/1.2095485
12. Lee CH, Kuo CV, Lee CL (1989) Thin Solid Films 173:59. doi:10.1016/0040-6090(89)90537-3
13. Damodara Das V, Kirupavathy S, Damodare L, Lakshminarayan N (1996) J Appl Phys 79:8521. doi:10.1063/1.362477
14. Korobov V, Leibovitch M, Shapira Y (1994) Appl Phys Lett 65:2290. doi:10.1063/1.112721
15. Armstrong NR, Lin AMC, Kuwana T (1976) Anal Chem 48:741. doi:10.1021/ac60368a035
16. Duncan SJ, Burstein GT (1987) J Appl Electrochem 17:196. doi:10.1007/BF01009146
17. Salem TM, Ismail AA (1970) J Chem Soc A:2415. doi:10.1039/j19700002415
18. Saidman SB, Bellocq EC, Bessone JB (1990) Electrochim Acta 35:329. doi:10.1016/0013-4686(90)87006-N
19. Omanovic S, Metikos-Hukovic M (1995) Solid State Ion 78:69. doi:10.1016/0167-2738(95)00009-U
20. Weiher RL, Ley RP (1966) J Appl Phys 37:299. doi:10.1063/1.1707830
21. Masato M, Kazuma M, Takeshi S, Toshiaki O (2002) Corros Sci 44:887. doi:10.1016/S0010-938X(01)00094-4
22. El-Sayed A, Shaker AM, Gad El-Kareem H (2003) Bull Chem Soc Jpn 76:1527. doi:10.1246/bcsj.76.1527
23. El-Sherbini EEF, Abd El-wahab SM, Amin MA, Deyeb MA (2006) Corros Sci 48:1885. doi:10.1016/j.corsci.2005.08.002
24. Xiaolong Z, Sandenbergh RF (2001) Mater Corros 52:685. doi:10.1002/1521-4176(200109)52:9<685::AID-MACO685>3.0.CO;2-H
25. Abdel Rehim SS, Sayyah SM, El Deeb MM (2003) Mater Chem Phys 80:393. doi:10.1016/S0254-0584(03)00128-7

26. El-Sayed A, Abd El-Rehim SS, Mansour H (1991) Monatsh Chem 122:1019. doi:10.1007/BF00811110
27. Abd El Rehim SS, Zaky AM, Mohamed NF (2006) J Alloy compd 424:88
28. Abd El-Rehim SS, Hassan HH, Mohamed NF (2004) Corros Sci 46:1071. doi:10.1016/S0010-938X(03)00134-3
29. Thanh PT, Akiyama A, Saji T (1982) Electrochim Acta 27:847. doi:10.1016/0013-4686(82)80206-5
30. Lee JG, Mori H, Yasuda H (2002) Phys Rev B 65:132106. doi:10.1103/PhysRevB.65.132106
31. Chu S, Yanar C, Schwartz A, Massalski J, Laughlin TB (2005) International Conference on Solid–Solid Phase, 22